

**QUANTIFICATION OF AVAILABLE WATER CONTENT COMPARING
STANDARD METHODS AND THE PEDOSTRUCTURE CONCEPT ON FOUR
DIFFERENT SOILS**

A Thesis

by

JOHN K BLAKE

Submitted to the Office of Graduate and Professional Studies of
Texas A&M University
in partial fulfillment of the requirements for the degree of

MASTER OF SCIENCE

Chair of Committee,	Rabi Mohtar
Committee Members,	Cristine Morgan
	Ralph Wurbs
	Erik Braudeau
	Amjad Assi
Head of Department,	Robin Autenrieth

December 2016

Major Subject: Civil Engineering

Copyright 2016 John K Blake

ABSTRACT

The purpose of this study is to evaluate the use of the pedostructure soil concept to determine the available water within soil. Specifically, the hydro-structural behavior of the soil in the pedostructure is compared to standard methods of determining field capacity and permanent wilting point. The standard methods evaluated are: the FAO texture estimate, Saxon and Rawls' pedotransfer functions, and the pressure plate method. Additionally, there are two pedostructure methods that are assessed: the water retention curve (WRC) and the soil shrinkage curve (ShC) methods. Three different types of soils were used: 1) Loamy Fine Sand: Undisturbed cores: Millican, Texas, USA; 2) Silty Loam: Reconstituted cores: Versailles soil, France; and 3) Silty clay loam: Reconstituted cores, Rodah Soils, Qatar. The results showed that the water contents at specific water potentials, empirically suggested values, of 330 hPa and 15,000 hPa for estimating the field capacity and permanent wilting point, respectively the three standards methods and the pedostructure WRC method were in relative agreement. On the other hand, the ShC method used transition characteristic points in the shrinkage curve to estimate the field capacity and permanent wilting point and was significantly higher. For example, in the fine sandy loam Ap horizon analyzed in this study, the field capacity estimates by standard and WRC methods ranged from 0.073 to 0.150 m³_{H₂O}/m³_{soil} while the ShC method estimate was 0.342 m³_{H₂O}/m³_{soil}. Overall, it is evident that the process of extracting parameters from the ShC that correlate to the field capacity point of a soil always results in a larger amount of available water. One potential reason for the higher values could be in the selection of

the transition point that represents the field capacity. Therefore, it is suggested to have further research to identify the most suitable characteristic point on the shrinkage curve to represent the field capacity value.

ACKNOWLEDGEMENTS

I would like to thank my committee chair, Dr. Mohtar, and my committee members, Dr. Morgan, Dr. Wurbs, Dr. Braudeau, and Dr. Assi for their commitment and support throughout the course of this research. There is no way that I would have been able to do this without the guidance, encouragement, and knowledge of my committee members.

Thanks also go to my friends and colleagues and the department faculty and staff for making my time at Texas A&M University a great experience. I also want to extend my gratitude to the Water Scholars Program and the Texas Water Resources Institute Mills Scholarship for their belief in my research and their financial assistance.

Finally, thanks to my parents for giving me the foundation to be able to excel in the academic world and for the character qualities that they have instilled in me. And of course, thanks to my wife for her constant encouragement, love, and hard work to help me realize my goals and aspirations.

CONTRIBUTORS AND FUNDING SOURCES

Contributors

This work was supported by a thesis committee consisting of Dr. Rabi Mohtar (advisor) and Dr. Ralph Wurbs of the Department of Civil Engineering and Dr. Cristine Morgan of the Department of Soil and Crops Sciences. Additionally, Dr. Erik Braudeau and Dr. Amjad Assi of the Department of Biological and Agricultural Engineering were special appointment committee members.

The data analyzed in Chapter 4 was gathered from an article published by Braudeau et al in 2014.

All work for the thesis was completed by the student, under the advisement of Dr. Rabi Mohtar of the Department of Civil Engineering and Dr. Erik Braudeau, and Dr. Amjad Assi of the Department of Biological and Agricultural Engineering.

Funding Sources

Graduate study was supported by a fellowship from the Texas Water Resources Institute, the Mills Scholarship Water Scholars Scholarship, and the Haynes '46 Fellowship.

TABLE OF CONTENTS

	Page
1. INTRODUCTION AND LITERATURE REVIEW	1
1.1 Background	1
1.2 Objectives	5
2. PROBLEM	7
2.1 Introduction.....	7
2.2 Theoretical Background.....	9
2.2.1 Defining Available Water	9
2.2.2 Standard Techniques for Calculating AW	10
2.2.3 Pedostructural Methods.....	16
2.2.4 Bulk Density.....	27
2.2.5 Establishing Reference Values.....	29
3. MATERIALS AND METHODS	30
3.1 Sample Collection and Preparation.....	30
3.2 Soil Characterization Laboratory Measurements	32
3.3 Finding Bulk Density.....	33
3.4 Measuring Shrinkage Curve and Water Retention Curve.....	33
3.5 Determination of Hydro-Structural Parameters	34
3.6 Quantification of Available Water.....	34
4. RESULTS AND DISCUSSION	35
4.1 Comparison of Techniques	35
4.2 Varying Bulk Density	45
4.3 Summary of the Methods Used.....	47
5. CONCLUSIONS	49
REFERENCES	51

LIST OF FIGURES

	Page
Figure 1	Diagram showing the available water for different textures of soil 1
Figure 2	ShC and WRC example from TypoSoil data 3
Figure 3	Shrinkage curve indicating micro and macro water contents 17
Figure 4	Water retention curve indicating water pools 19
Figure 5	Available water comparison for MR-Ap 38
Figure 6	Available water comparison for MR-E soil 39
Figure 7	Available water comparison for Rodah 39
Figure 8	Available water comparison for Versailles 40
Figure 9	MR-Ap shrinkage curves used with average WL and WN plotted 41
Figure 10	MR-Ap water retention curves with average FC and WP plotted 41
Figure 11	MR-E soil shrinkage curves with average WL and WN plotted 42
Figure 12	MR-E water retention curves with average FC and WP plotted 42
Figure 13	Rodah soil shrinkage curves with average WL and WN plotted 43
Figure 14	Rodah water retention curves with average FC and WP plotted 43
Figure 15	Versailles soil shrinkage curve with WL and WN plotted 44
Figure 16	Versailles water retention curve with FC and WP plotted 44

LIST OF TABLES

	Page
Table 1	FAO soil water characteristics for different textures (modified (1998)).....11
Table 2	Description of 12 state variables (hydro-structural parameters) 21
Table 3	Wet and dry specific volume and bulk density for all four soil types.....35
Table 4	MR-Ap soil samples summary of five methods..... 37
Table 5	MR-E soil samples summary of five methods 37
Table 6	Rodah soil samples summary with averages and standard deviations 38
Table 7	Versailles soil sample summary with averages and standard deviations 38
Table 8	Impact of using a constant bulk density vs. wet and dry bulk destiny 46
Table 9	Comparison of strengths and weaknesses 48

1. INTRODUCTION AND LITERATURE REVIEW

1.1 Background

For decades, soil scientists and irrigation engineers have sought to understand the plant-soil-water interactions within a soil medium, specifically, to establish an accurate measurement of the water holding capacity of soil. This capacity is commonly referred to as the “available water” (AW) within the soil. There are specific states of soil moisture that play important roles in agronomic irrigation management: in particular, field capacity,

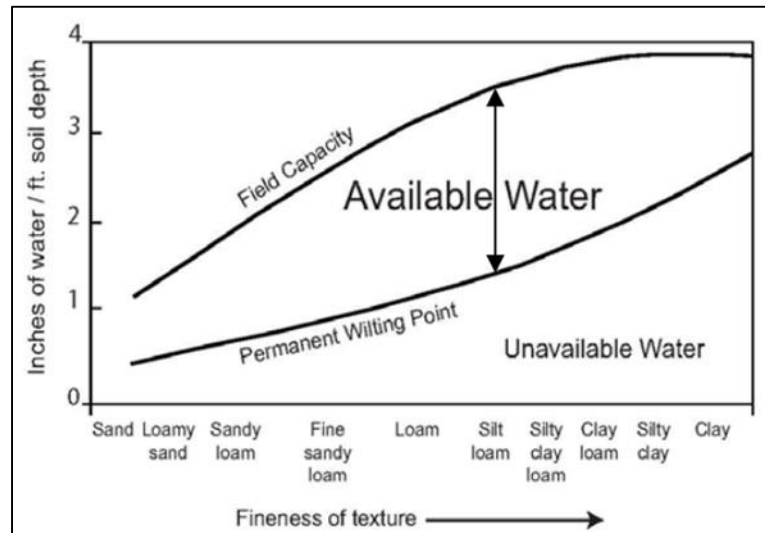


Figure 1: Diagram showing the available water for different textures of soil (USDA, 2008)

the optimal quantity of water within the soil for plants to extract, and permanent wilting point, the point at which the plant can no longer extract water and begins to die or wilt. By subtracting the permanent wilting point moisture content from the field capacity, the available water can be found (figure 1). Many different methods have been used to

estimate these two vital soil moisture contents. In most cases, these contents have been determined based on empirically derived values of soil water retention. The field capacity moisture state is generally, in the agronomic world, to be between 100-330 hPa while the permanent wilting point is typically set at 15,000 hPa (Singh, 2007). Two of the common methods to measure the water retention (both highlighted in this paper) are the pressure plate method (for high retention values $h > 1000$ hPa, a good estimation for the permanent wilting point) and the tensiometer method (for low retention values $h < 1000$ hPa, which is a good estimation for the field capacity). The pressure plate is a device, developed by Richards (1948), that is designed to measure soil moisture at particular internal water tension states by applying an external pressure. The tensiometer method consists of inserting a small porous cup into the soil and measuring the internal tension of the soil via a pressure transducer (the tensiometer) (Richards, 1941; Richards and Gardner, 1936). These tension readings, in combination with water content data, are used to create the water retention curve (WRC). As it is known, the measuring range of tensiometers are limited up to 800-1000. However, Braudeau et al., (2014a) showed that the water retention curve can be extended to allow for readings greater than the 800-1000 hPa range that is measured by the tensiometer, their methodology for finding values higher than 1000 hPa on the WRC will be explained below.

Although widely accepted, these standard techniques of finding field capacity and permanent wilting point are based on set values of water retention (330 hPa and 15000 hPa) that have limited explanation in literature for why they were chosen; they both fail to explain whether or how they take into account the soil aggregates structure which plays

a pivotal role in understanding the water storage and flow within the soil medium. Another method commonly used is an experimentally based range for the permanent wilting point

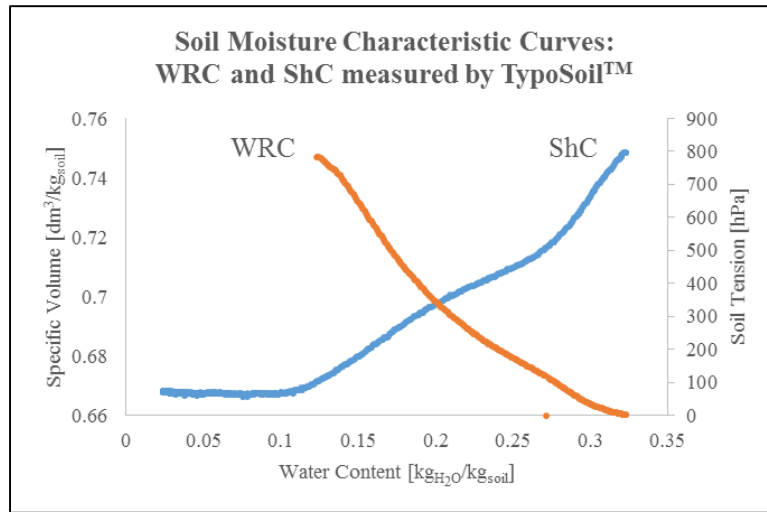


Figure 2: ShC and WRC example from TypoSoil data

and field capacity based on soil texture. The Food and Agriculture Organization of the United Nations (FAO) built an extensive list compiling a range of values for both field capacity and permanent wilting point of different soil textures (Allen et al., 1998). Building on the texture and water retention approaches, Saxton and Rawls developed pedotransfer equations that took into account sand, clay, and organic matter content to estimate soil moisture at field capacity (330 hPa) and permanent wilting point (15,000 hPa) (Saxton & Rawls, 2006). Although Saxon and Rawls begin to diverge into the specific characteristics of the soil, their equations are designed to simply predict the soil moisture at 330 hPa and 15,000 hPa, leaving those same issues that arise in the texture and

water retention methods untouched. Each of the four mentioned methods explore different techniques to find the water content at 330 hPa and 15,000 hPa.

Following the work of Braudeau et al. (2004, 2009), Braudeau et al. (2014b) developed thermodynamically-based equations for water retention curve (WRC) and soil shrinkage curve (ShC) so as to characterize the aggregates structure of the soil medium (defined as the pedostructure) and how it interacts with water. The ShC shows the change in the volume of the soil column as water is removed; whereas, the WRC indicates the change in water potential, or retention, within the soil as water leaves the system (Figure 2). In these equations of the WRC and ShC, the state variables namely: water content, volume, and retention and the characteristic parameters were referenced to the fix dry mass of the soil pedostructure, represented by the dry mass of a soil core. The parameters of these thermodynamic equations are characteristic of the two characteristic curves and in many cases represents transition points in the curves. Therefore, it is very important to have accurate continuous data measurements to capture these important transition points. Fortunately, Bellier and Braudeau (2013) developed an apparatus (TypoSoil™) that can simultaneously and continuously measure the mass, diameter, height, and pressure within the soil sample to create these two curves. Saturated soil samples with diameters and heights of 5 cm are used. Within the device, there are separate mechanisms that allow for measurement of the four quantities needed for modeling the two curves. The inner-workings and operation of the TypoSoil™ can be found in Assi et al. (2014). The curves are then modeled using the thermodynamically derived equations to find the hydro-structural parameters that represent specific measurable physical properties of the soil.

Consequently, the major advantage to this process is that the curves can be modeled by using physical characteristic parameters. Thus, when a given parameter changes, it is easy to identify what was altered within the soil medium.

Even with this novel approach for determining the hydro-structural properties of the soil, there remains a gap in applicability when attempting to compare with standard methods of determining soil moisture. The ability to apply the theoretical laboratory concepts to the field begins with interpreting the parameters extracted from the TypoSoil™ outputs into something useful to agricultural development. This starts with quantifying the water held within the soil yet accessible to the plant, commonly referred to as “available water” (AW). The AW is completely dependent upon the soil characteristics, usually soil texture (% sand, % clay) and percentage of organic matter by weight (Saxton and Rawls, 2006). The clay content, type and the organic matter play impetrative role in forming the soil aggregation and structure. Given this fact, identifying certain hydro-structural parameters of these aggregates can be used as a quantitative tool to identify the field capacity and permanent wilting point. After identification, it becomes possible to compare the pedostructure field capacity and permanent wilting point with other standard methods of determining AW.

1.2 Objectives

The general objective of this research is to more accurately quantify the available water for plant use. This will be done by highlighting the limitations of current understanding related to the quantification process of available water and then presenting

a new approach to overcome these shortcomings, addressing three specific objectives, as follows:

- (1) Develop a quantitative methodology to estimate available water using the pedostructure concept.
- (2) Demonstrate the application on different soil types
- (3) Compare the standard methods of quantifying available water with the pedostructural methods and discuss strengths and weaknesses of each.

2. PROBLEM

2.1 Introduction

Quantifying soil water holding capacity has always been a fundamental aspect of irrigation water management. In this chapter, the range of soil moisture that can be stored in soil and be available for plant use will be referred to as the available water (AW). Therefore, AW can be calculated by subtracting the soil moisture content at permanent wilting point (PWP) from the moisture content at field capacity (FC). These two contents are the foundation of soil-water availability to plants. However, solutions for determining them have been abundantly diverse and inconsistent. Although the importance of AW is rarely questioned, the ways in which it is quantified have been debated regarding both accuracy and reliability. This chapter focuses on the limitations of current understandings related to quantifying AW and presents a new approach to provide better definition and quantification of these values by considering the soil aggregates structure and their thermodynamic interaction with water.

Over the years, many different methods have been developed to measure the quantity of AWC. This chapter will look at some of the most popular, widely used methods for quantifying FC and WP with the goal of understanding current practices and the accuracy of the techniques employed, as well as to introduce a new concept based on soil aggregation, referred to here as the *pedostructural method*. In this study, we can divide the research into two groups based on the method used and compared, and the soil and cores types: in the first group, 8 undisturbed soil cores were sampled from: Ap horizon (4 replicates), and E horizon (4 replicates) from a local farm in Millican, Texas and analyzed

by TypoSoil to construct the water retention curve, and soil shrinkage curve. Then, one undisturbed soil core measuring 50 cm from the top soil (how many and what are they) was sent to the Texas A&M Soil Characterization Laboratory to identify the soil texture (% sand, % clay, % silt), the organic matter. To determine the particle size distribution and organic matter content, the core was ground and sieved to 2 mm. Additionally, the ground and sieved soil was analyzed by using the pressure plate, to get the water content at 330 hPa and 15000 hPa. The soil texture, % sand, % clay, % OM and the pressure plate measurements then used to calculate the field capacity and permanent wilting point using the three standard methods: i) FAO texture estimate, ii) Pedotransfer functions utilizing measured values from the laboratory, iii) pressure plate laboratory measurement; whereas, TypoSoil measurements enable the use of pedostructural methods: iv) water retention curve (WRC) method depending on the internal pressure measurements, and v) soil shrinkage curve (ShC) method using extracted hydro-structural properties of the soil. Each of these methods (standard methods and pedostructural methods) will be explained in details in the following sections. The soil samples of Ap and E horizons are high in sand concentration and, consequently, have very little structure and shrinkage, which affected the applicability of the shrinkage curve method. Therefore, a second group of soil samples were used to be able to compare with the shrinkage curve method. For this purpose, the characteristic curves of two previously studied and published soils were used. The soil samples used in these studies were reconstituted soil samples: Rodah soil, silty clay loam soil from Qatar (Assi et al., 2014), and Versailles soil, silty loam soil from France (Erik Braudeau et al., 2014b). For the Rodah and Versailles soils, only the water retention curve

and soil shrinkage curve were calculated and used to compare with the FAO estimate. In these published data, there was no information about the organic matter content and the pressure plate measurements, therefore, the pedotransfer function and pressure plate methods were not used in the comparison of the second group.

2.2 Theoretical Background

2.2.1 *Defining Available Water*

In order to compare these five methods, a clear definition of available water (AW) must be established. Water within the soil is controlled by the capillary action resulting from the adhesive properties of water and soil. In order for the water to be available, the adhesive force between the water and the soil must be greater than the force exerted by the gravity that pulls the water downwards (Singh, 2007). It is commonly acknowledged among soil scientists and agronomists that the point at which all the gravitational water has drained from the soil is called the field capacity (FC). At this point, the plant has the maximum quantity of AW for extraction and has been widely accepted to have an internal soil suction of 100 hPa for coarse textured soils or of 330 for fine soils (Singh, 2007). Of course, this amount differs with respect to the characteristics of the soil. Additionally, the lower limit of water availability or the permanent wilting point (PWP), is heavily dependent upon the type of soil, particularly soil texture % sand, % clay (FAO, 1998), and also organic matter (Saxon and Rawls, 2006). The permanent wilting point (PWP) is defined as the point at which the plant can no longer extract water and begins to die or wilt and will not recover. At this point the adhesion forces between the soil and water are greater than the suction force of the plant. This soil-water quantity is generally accepted

to be the point at which an external pressure of -15 bar (15,000 hPa) is applied (Singh, 2007). Therefore, the water content retained within the soil between the FC and the WP can also be referred to as the available water (AW). Thus, the equation is simply:

$$AW = \theta_{FC} - \theta_{PWP} \quad [1]$$

where θ_{FC} and θ_{PWP} are the volumetric water contents at field capacity and permanent wilting point, respectively [$\text{m}^3_{\text{H}_2\text{O}}/\text{m}^3_{\text{soil}}$]. A distinction must be made between what FAO refers to as the Total Available Water (TAW) and what we will call available water (AW) in this chapter (Allen et al., 1998). The TAW that referenced by FAO takes into account the root depth and is therefore simply AW multiplied by the depth of the root. Thus, Allen et al. (1998) derived TAW as equation [2]:

$$TAW = (\theta_{FC} - \theta_{PWP})Z_r \quad [2]$$

where TAW is the total available water [mm], and Z_r is equal to the root depth [mm]. For the purposes of this chapter, the rooting depth will be ignored and the definition of soil AWC will be stated as equation [1]. With AWC clearly defined, the variables and methods for determining available water must be discussed.

2.2.2 Standard Techniques for Calculating AW

The different methods for finding field capacity and permanent wilting point can be split into two categories: standard and pedostructural techniques. Standard methods include the FAO texture estimate, Saxon and Rawls' Pedotransfer functions, and the pressure plate method.

FAO Estimate Method

With FAO's abundant resources, it was possible to experimentally calculate the volumetric water content at field capacity and permanent wilting point for the entire range of soil textures, from sand to clay (table 1) (Allen et al., 1998). The advantage of this resource is that a laboratory is not needed to estimate available water. However, it can only provide a rough estimate: although the FAO measurements are very robust, reported

Soil Type	θ_{FC} (m^3/m^3)	θ_{WP} (m^3/m^3)
Sand	0.07-0.17	0.02-0.07
Loamy Sand	0.11-0.19	0.03-0.10
Sandy Loam	0.18-0.28	0.06-0.16
Loam	0.20-0.30	0.07-0.17
Silt Loam	0.22-0.36	0.09-0.21
Silt	0.28-0.36	0.12-0.22
Silt Clay Loam	0.30-0.37	0.17-0.24
Silty Clay	0.30-0.42	0.17-0.29
Clay	0.32-0.40	0.20-0.24

Table 1: FAO soil water characteristics for different textures (modified (1998))

results can only offer a range of values for FC and WP for each texture. This is mostly due to the fact that soil can have different properties, even if classified in the same texture class due to diversity in physical, chemical, or biological properties. For instance, biological properties, mainly organic matter, play pivotal role in improving soil aggregation and structure and its water holding capacity (Hudson, 1994); therefore, it is possible to have two soil with the same texture but having different aggregates structure, and hence different hydro-structural properties. This limitation significantly restricts the potential of

using these values to accurately model and calculate the AWC. Allen et al. (1998) do not provide clear directions choosing values in the range depending on the soil texture, therefore and in most cases, it is necessary to either make an “educated guess” or to use the average value. As mentioned, the only basis for choosing a given range is the soil texture. This can create quite a few problems in that it fails to take into account the aggregation of the soil and other physical, chemical, or biological properties of the soil. For the purposes of this study the average value used in FAO method will be based on the texture of the soil used as a sample.

Pedotransfer Function Method

Many scientists and engineers have attempted to expand upon the texture approach of estimating water content by using other physical or chemical properties of the soil. Most of the theories developed are based on statistical results that lead to functions that can estimate water content based on the soil’s characteristics. These functions have come to be known as pedotransfer functions. The purpose of creating pedotransfer functions is to estimate the hydraulic properties of a soil by using its unique characteristics. Over the years, many different functions have been developed that have attempted to accurately measure this relationship. Although there is a considerable variability in the reliability of each function, the most commonly used set of equations were derived by Saxton and Rawls (2006). Their equations take into account particle size distribution (sand and clay percentages) and the organic matter in determining the soil water content at field capacity (330 hPa) and permanent wilting point (15,000 hPa). A clarifying statement is needed in that Saxon and Rawls state that sand, clay, and organic matter quantities should be entered

in percent weight, but in reality these values should be in decimal form, such that the units are $\text{kg}_{\text{sand}}/\text{kg}_{\text{total}}$, $\text{kg}_{\text{clay}}/\text{kg}_{\text{total}}$, and $\text{kg}_{\text{OM}}/\text{kg}_{\text{total}}$ respectively. The field capacity estimation was derived such that:

$$\theta_{33} = \theta_{33t} + [1.283(\theta_{33t})^2 - 0.374(\theta_{33t}) - 0.015] \quad [3]$$

$$\begin{aligned} \theta_{33t} = & -0.251S + 0.195C + 0.0110M + 0.006(S \times OM) \\ & - 0.027(C \times OM) + 0.452(S \times C) + 0.299 \end{aligned} \quad [4]$$

Where θ_{33} is the volumetric water content at 33 kPa (field capacity) with normal density [$\text{m}^3_{\text{H}_2\text{O}}/\text{m}^3_{\text{soil}}$], θ_{33t} is the first solution of the soil moisture at 33 kPa [$\text{m}^3_{\text{H}_2\text{O}}/\text{m}^3_{\text{soil}}$], S is the percent of sand particles by mass [$\text{kg}_{\text{sand}}/\text{kg}_{\text{total}}$], C is the percent of clay particles by mass [$\text{kg}_{\text{clay}}/\text{kg}_{\text{total}}$], and OM is the percent of organic matter by mass [$\text{kg}_{\text{OM}}/\text{kg}_{\text{total}}$]. Similarly, the permanent wilting point can be estimated using equations [5] and [6].

$$\theta_{1500} = \theta_{1500t} + (0.14 \times \theta_{1500t} - 0.02) \quad [5]$$

$$\begin{aligned} \theta_{1500t} = & -0.024S + 0.487C + 0.006OM + 0.005(S \times OM) \\ & - 0.013(C \times OM) + 0.068(S \times C) + 0.031 \end{aligned} \quad [6]$$

Where θ_{1500} is the volumetric water content at 1500 kPa (permanent wilting point) with normal density [$\text{m}^3_{\text{H}_2\text{O}}/\text{m}^3_{\text{soil}}$], θ_{1500t} is the first solution of the soil moisture at 1500 kPa [$\text{m}^3_{\text{H}_2\text{O}}/\text{m}^3_{\text{soil}}$].

These are predictive equations with limited predictive accuracy based on statistical analysis. For example, the coefficient of determination (R^2) for θ_{33} and θ_{1500} are 0.63 and 0.86, respectively. This means that there is quite a bit of variability within this equation: results must be accepted with this uncertainty in mind. A reason for the limited accuracy could be the fact that these equations only take into account the percentages of different

physical elements of the soil but lack incorporation of the structural aggregation of the soil.

Pressure Plate Method

During the past century, soil scientists have discovered that the internal soil tension offers insight into the “water infiltration, redistribution, evaporation, plant water uptake, and microbial activity” of the soil (Bittelli and Flury, 2009). Therefore, many different techniques have been developed for finding the internal soil tension. It has become apparent that the most common method, by far, over the past 50 years has been the pressure plate method. This is due to its soundness of theory and relative accuracy (Richards, 1948). In this procedure, a completely saturated soil sample is placed inside a chamber, sealed except for the bottom, where a porous membrane exposed to atmospheric air pressure is found and upon which the sample is placed. At this point a positive pressure is applied to the chamber (15,000 hPa for WP and 330 hPa for FC) until equilibrium is reached across the membrane. After equilibrium is achieved, the sample is removed from the chamber and its mass recorded. Finally, the dry mass is determined, typically by placing the soil in an oven at 105° C for 24 hours and then weighing it immediately upon removal from the oven. Equations [7] and [8] can be used to calculate the specific water content [$\text{kg}_{\text{H}_2\text{O}}/\text{kg}_{\text{soil}}$] for field capacity and permanent wilting point, respectively.

$$\overline{W}_{FC} = \frac{M_{330} - M_s}{M_s}, \text{ and} \quad [7]$$

$$\overline{W}_{PWP} = \frac{M_{15000} - M_s}{M_s}, \quad [8]$$

where \overline{W}_{FC} and \overline{W}_{PWP} are the specific water contents at field capacity (330 hPa) and permanent wilting point (15,000 hPa), respectively [$\text{kg}_{\text{H}_2\text{O}}/\text{kg}_{\text{soil}}$], M_{330} and M_{15000} are the mass of the soil sample at 330 hPa and 15,000 hPa, respectively [$\text{kg}_{\text{H}_2\text{O}+\text{soil}}$], and M_s is the dry mass [kg_{soil}]. These equations can be converted to volumetric water contents using the following:

$$\theta_{FC} = \overline{W}_{FC} \left(\frac{\rho_t}{\rho_w} \right), \text{ and} \quad [9]$$

$$\theta_{PWP} = \overline{W}_{PWP} \left(\frac{\rho_d}{\rho_w} \right); \quad [10]$$

where θ_{FC} and θ_{PWP} are the volumetric water contents at field capacity and permanent wilting point, respectively [$\text{m}^3_{\text{H}_2\text{O}}/\text{m}^3_{\text{soil}}$], ρ_t and ρ_d are the wet and dry bulk density of the soil, respectively [$\text{kg}_{\text{soil}}/\text{m}^3_{\text{soil}}$] and ρ_w is the specific density of water [$\text{kg}_{\text{H}_2\text{O}}/\text{m}^3_{\text{H}_2\text{O}}$]. Typically, in the soil science community, the wet bulk density (or the bulk density at field capacity) is used to convert from gravimetric water contents to volumetric. And, ρ_d the dry bulk density is used for permanent wilting point calculation. Then, the difference between these two values represents the available water for soil.

Similar to the texture and pedotransfer function methods for determining water content, the pressure plate depends on the same assumption of the water potential limits of 330 hPa and 15000 hPa for field capacity and permanent wilting point, respectively. The major shortcoming of this method is related to the accuracy of measurements at field capacity which is more significant than the permanent wilting point in determining the AW. Actually, the accuracy of pressure plate measurements at low water retention has been questioned (Schelle, et al., 2013).

2.2.3 *Pedostructural Methods*

This is where the theory of soil pedostructure comes in. Assi et al., (2014) and Braudeau et al., (2014b) couple the water retention curve (WRC) with the soil shrinkage curve (ShC) to calculate the hydro-structural parameters relating to the soil-water storage and interaction. In order to evaluate the soil characteristics using the pedostructure concept, the water retention and shrinkage characteristic curves are necessary. There are two main reasons for determining these characteristic curves by having simultaneous and continuous measurements of water, content, volume and retention: 1) to capture the inflection points and transition zones in order to delineate the soil aggregate organization and 2) to develop accurate estimates for the hydro-structural parameters. Both of these objectives can only be accomplished using simultaneous and continuous measurements provided by TypoSoil™ (Bellier and Braudeau, 2013) that then allow the data to be fitted to the thermodynamically-based equations. (Assi et al., 2014; Braudeau and Mohtar, 2014; Braudeau et al., 2014a,b; Braudeau et al., 2016).

Data collected from the TypoSoil™ can be used to determine the specific volume, \bar{V} , and the specific water content, \bar{W} of the sample. In order to calculate these two important factors, assumptions had to be made such as isotropic radial shrinkage and uniform distribution of the water content within the soil medium. With these assumptions, the following equations ([11] and [12]) can be used to find the specific volume and water content:

$$\bar{V} = \frac{\pi d^2 H}{4M_s} \quad [11]$$

where \bar{V} is the specific volume of the soil sample [$\text{dm}^3/\text{kg}_{\text{solid}}$], d is the diameter of the sample [dm], H is the height [dm], and M_s is the dry mass of the sample after 48 hours of drying at 105°C [kg_{solid}].

$$\bar{W} = \frac{m - M_s}{M_s} \quad [12]$$

where \bar{W} is the specific water content [$\text{kg}_{\text{H}_2\text{O}}/\text{kg}_{\text{soil}}$], and m is the measured mass of the soil sample [$\text{kg}_{\text{H}_2\text{O}}$]. These two equations, along with internal tension measurements, can be used to create the ShC and WRC.

The soil shrinkage curve (ShC) has four phases that constitute the entire shrinkage

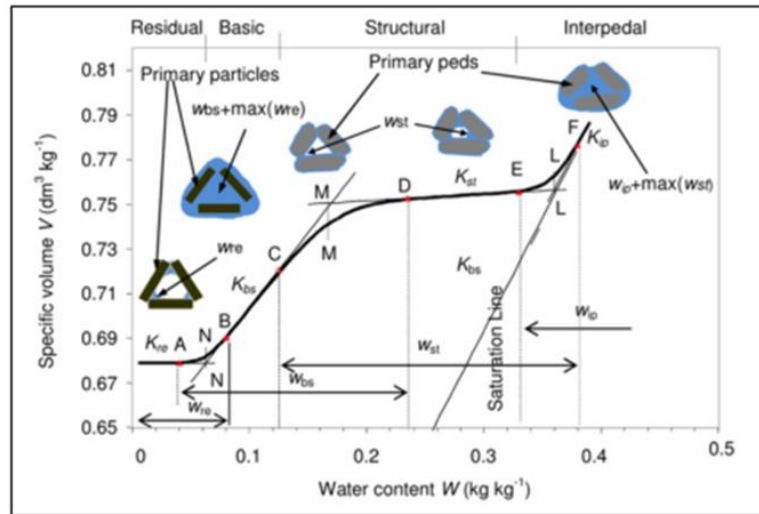


Figure 3: Shrinkage curve indicating micro and macro water contents

portfolio: interpedal, structural, basic, and residual (Figure 3). Identifying these various phases allows for an accurate model of the curves. Interpedal water is the moisture present outside of the primary peds and largely controlled by gravitational forces. Primary peds,

as defined by Brewer (1964), are the simplest peds occurring in a soil material; that cannot be divided into smaller peds, but they may be packed together to form compound peds of higher level of organization. Therefore, Primary peds can be considered as the first functional level of organization in a soil medium. The structural water, like the interpedal, is also located outside the primary peds, but the thermodynamics of the soil-water interactions, mostly adhesion forces, have taken over primary control of water movement. The combination of interpedal water and structural water constitutes the entire water content outside of the primary peds, and will be referred to in this paper as the “macro” water. The basic water “pool” is where the most soil shrinkage potential exists. It is located inside the primary peds. Lastly, the residual water is that which is left over after all the accessible water within the soil has been evaporated, where the volume of the soil remains rigid although the soil water is drained out. Both basic and residual water is controlled by the capillary action from the water and the soil’s adhesive properties within the primary peds. Together, these are referred to as the “micro” water. Between each of these phases there are fundamental transition points labeled N, M, and L, from left to right or lower to higher water contents. The water content at point N represents the dry state inside the primary peds or dry micropores. Point M signifies saturated micropores and point L is the transition point of water content between interpedal water exiting the soil medium and the thermodynamics taking over control.

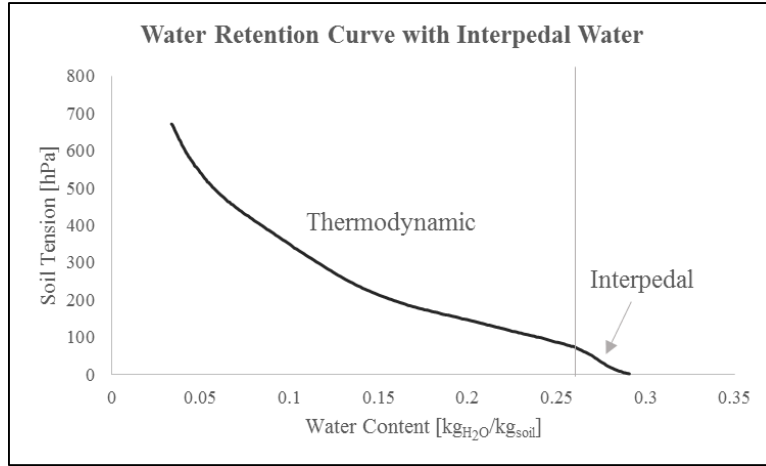


Figure 4: Water retention curve indicating water pools

Similarly, the water retention curve can be split into two major water pools (figure 4). The interpedal water, if present, creates one portion of the curve and behaves differently than the section of the curve that is made up of the structural, basic, and residual water. In the majority of cases, the tension of the soil reaches the breaking point of the tensiometer before entering the residual, or even, the basic phase of water content. Therefore, to find the tension of the soil while in the residual or basic phase, there should be a way to extend the retention curve at these high water retention values beyond the measuring limits of tensiometers. Braudeau et al., (2014a) provide a thermodynamic-based equation to extend the water retention curve, this equation will be explained below.

After the creation of the ShC and WRC from raw data, state functions derived by Braudeau et al. (2014) can be used to model the two curves. These modeled curves are composed of 12 state variables which, for the purposes of this study, will be called hydro-structural parameters: \bar{W}_{miSat} , \bar{W}_{maSat} , \bar{E}_{mi} , \bar{E}_{ma} , \bar{V}_0 , \bar{W}_N , k_N , K_{bs} , K_{st} , \bar{W}_L , k_L , K_{ip} . The meaning of these parameters, what they represents and their physical units are explained

in Table 2. Note, the difference between variables with a bar above them and those without (e.i. \bar{W}_L vs W_L) is that the former is specific water content, meaning mass of the water divided by dry soil mass [$\text{kg}_{\text{H}_2\text{O}}/\text{kg}_{\text{soil}}$], and the latter is simply the mass of the water [$\text{kg}_{\text{H}_2\text{O}}$]. For example, \bar{W}_L is the specific water content (gravimetric water content) equivalent to W_L/M_d where M_d is the dry mass of the soil. With these definitions set, the next step is to define the equations for the ShC and the WRC. Equation 13 is the derivation of the ShC (Braudeau et al., 2014b):

$$\bar{V} = \bar{V}_0 + K_{bs}\bar{w}_{bs}^{eq} + K_{st}\bar{w}_{st}^{eq} + K_{ip}\bar{w}_{ip} \quad [13]$$

where \bar{V} is the specific volume of the soil sample [$\text{dm}^3/\text{kg}_{\text{soil}}$], \bar{V}_0 is the specific volume of the sample at the end of the residual phase (Figure 2) [$\text{dm}^3/\text{kg}_{\text{soil}}$], K_{bs} , K_{st} , and K_{ip} are the slopes of the basic, structural, and interpedal linear shrinkage phases, respectively [$\text{dm}^3/\text{kg}_{\text{H}_2\text{O}}$], and \bar{w}_{bs}^{eq} , \bar{w}_{st}^{eq} , and \bar{w}_{ip} are the specific water pools corresponding to the linear shrinkage phases of the pedostructure [$\text{kg}_{\text{H}_2\text{O}}/\text{kg}_{\text{soil}}$] and can be defined by the following equations ([14], [15], and [16]):

$$\bar{w}_{bs}^{eq} = \bar{W}_{mi}^{eq} - \bar{w}_{re} = \frac{1}{k_N} \ln[1 + \exp(k_N(\bar{W}_{mi}^{eq} - \bar{W}_{miN}^{eq}))] \quad [14]$$

$$\bar{w}_{st}^{eq} = \bar{W}_{ma}^{eq} = \bar{W} - \bar{W}_{mi}^{eq} \quad [15]$$

$$\bar{w}_{ip} = \frac{1}{k_L} \ln[1 + \exp(k_L(\bar{W} - \bar{W}_L))] \quad [16]$$

where \bar{W} is the total pedostructure water content [$\text{kg}_{\text{H}_2\text{O}}/\text{kg}_{\text{soil}}$], \bar{W}_{mi}^{eq} is the micropore water content inside the primary peds [$\text{kg}_{\text{H}_2\text{O}}/\text{kg}_{\text{soil}}$], \bar{W}_{ma}^{eq} is the macropore water content outside

the primary pedes [kg_{H₂O}/kg_{soil}] (see equations [17a] and [17b] for definitions of \overline{W}_{mi}^{eq} and \overline{W}_{ma}^{eq}), and \overline{W}_{miN}^{eq} is the micropore water content calculated by equation [17a] but using \overline{W}_N instead of \overline{W} , k_N and k_L represent the vertical distance in kg_{soil}/kg_{H₂O} between the intersection points of N-N' and L-L', respectively, on the shrinkage curve (Figure 2).

The micropore and macropore water contents were derive such that:

Parameter	Units	Description
W_{miSat}	kg _{H₂O}	The water content when the micropores are at saturation.
W_{maSat}	kg _{H₂O}	The water content when the macropores are at saturation.
\overline{E}_{mi}	J/kg _{soil}	The potential energy on the surface of the micropores.
\overline{E}_{ma}	J/kg _{soil}	The potential energy on the surface of the macropores.
\overline{V}_0	dm ³ /kg _{soil}	The specific volume when there is no observable change in water content.
W_N	kg _{H₂O}	The water content when the primary pedes are dry.
k_N	kg _{soil} /kg _{H₂O}	The vertical distance between N and N'.
K_{bs}	dm ³ /kg _{H₂O}	The slope of the basic shrinkage phase of the ShC.
K_{st}	dm ³ /kg _{H₂O}	The slope of the structural shrinkage phase of the ShC.
W_L	kg _{H₂O}	The water content when all interpedal water has drained.
k_L	kg _{soil} /kg _{H₂O}	The vertical distance between L and L'.
K_{ip}	dm ³ /kg _{H₂O}	The slope of the interpedal shrinkage phase of the ShC.

Table 2: Description of 12 state variables (hydro-structural parameters). One can refer to Figure 3 for better understanding of the transition points mentioned in the table

$$\overline{W}_{mi}^{eq}(\overline{W}) = \overline{W} - \overline{W}_{ma}^{eq} = \frac{\left(\overline{W} + \frac{\overline{E}}{A}\right) + \sqrt{\left[\left(\overline{W} + \frac{\overline{E}}{A}\right)^2 - \left(4 \frac{\overline{E}_{ma}}{A} \overline{W}\right)\right]}}{2} \quad [17a]$$

$$\overline{W}_{ma}^{eq}(\overline{W}) = \frac{\left(\overline{W} - \frac{\overline{E}}{A}\right) - \sqrt{\left[\left(\overline{W} + \frac{\overline{E}}{A}\right)^2 - \left(4 \frac{\overline{E}_{ma}}{A} \overline{W}\right)\right]}}{2} \quad [17b]$$

where $A = \frac{\overline{E}_{ma}}{\overline{W}_{maSat}} - \frac{\overline{E}_{mi}}{\overline{W}_{miSat}}$, in which \overline{W}_{maSat} and \overline{W}_{miSat} are the macro and micro water content at saturation so that $\overline{W}_{Sat} = \overline{W}_{maSat} + \overline{W}_{miSat}$ [kg_{H₂O}/kg_{soil}], and $\overline{E} = \overline{E}_{mi} + \overline{E}_{ma}$, where \overline{E}_{mi} [J/kg_{soil}] is the potential energy of the surface charges on the inner surface of the primary peds and, similarly, \overline{E}_{ma} is the potential energy of the surface charges on the outer surface of the primary peds [J/kg_{soil}]. Finally, the WRC was derived to create equation [18]:

$$h^{eq}(\overline{W}) = \begin{cases} h_{mi}(\overline{W}_{mi}^{eq}) = \rho_w \overline{E}_{mi} \left(\frac{1}{\overline{W}_{mi}^{eq}} - \frac{1}{\overline{W}_{miSat}} \right), \\ h_{ma}(\overline{W}_{ma}^{eq}) = \rho_w \overline{E}_{ma} \left(\frac{1}{\overline{W}_{ma}^{eq}} - \frac{1}{\overline{W}_{maSat}} \right) \end{cases} \quad [18]$$

where h^{eq} is the soil suction at any water content (\overline{W}) [dm \approx kPa], h_{mi} is the soil suction within the primary peds [dm \approx kPa], h_{ma} is the soil suction outside of the primary peds [dm \approx kPa], and ρ_w is the specific density of water [1 kg_{H₂O}/dm³]. Equations [11]-[18] are used to model the raw data that create the ShC and WRC. After the modeling, the specific hydro-structural parameters can be extracted from the curves for application purposes.

Water Retention Curve Method

One solution that arises when using the pressure plate method is explained by Braudeau et al. (2014a) in that the internal tension of the soil and the positive pressure applied during the pressure plate method procedure are two distinct values. Although there is a distinction between the two, there is also a relationship, which is explained by the thermodynamic equilibrium of the soil-water retention and the applied pressure on soil, such that:

$$h = 137.72 \ln(\Pi/100 + 1) \quad [19]$$

where h is the water retention of the sample [kPa] and Π is the applied pressure at $T = 294$ K [kPa]. Given this relationship, Braudeau et al. (2014a) concludes that an applied pressure of 15,000 hPa is equivalent to 3,754 hPa of corresponding soil-water retention. This thermodynamically explains a fundamental issue, such that: if the field capacity is equivalent to the 330 hPa soil-water retention; then the permanent wilting point is equivalent to 3,754 hPa soil-water retention and *not* 15,000 hPa soil-water retention. The authors also showed that, at applied pressures less than 800 hPa the internal tension is the same as the applied external pressure (Braudeau et al., 2014).

The water retention of a soil can be measured by using a tensiometer placed in direct contact with the matrix of the soil. By collecting multiple measurements at different water contents, a water retention curve (WRC) can be formed. The WRC is simply the internal water tension [hPa] vs. specific water content [$\text{kg}_{\text{H}_2\text{O}}/\text{kg}_{\text{soil}}$]. An issue arises in that the most advanced tensiometer can only measure the water retention up to 800-1000 hPa while, as stated earlier, the permanent wilting point is not reached until 3,754 hPa. The

only way to find the water content at the permanent wilting point is to accurately model the WRC for the given data and extend it as needed. This process is what Braudeau et al. show to be possible in an additional paper (Braudeau et al., 2014a). Therefore, the water content at any water tension can be found by adding equations [20] and [21]:

$$\bar{W}_{mi} = \frac{10 \times \bar{E}_{mi}}{(h - h_{ip}) + (10 \times (\bar{E}_{mi}/\bar{W}_{miSat}))} \quad [20]$$

$$\bar{W}_{ma} = \frac{10 \times \bar{E}_{ma}}{(h - h_{ip}) + (10 \times (\bar{E}_{ma}/\bar{W}_{maSat}))} \quad [21]$$

where \bar{W}_{mi} and \bar{W}_{ma} are the micro and macro water content, respectively [$\text{kg}_{\text{H}_2\text{O}}/\text{kg}_{\text{soil}}$], \bar{E}_{mi} and \bar{E}_{ma} are constants representing the potential energy on the surface of the micropores and macropores respectively [$\text{J}/\text{kg}_{\text{soil}}$]; h is the water retention [hPa]; h_{ip} is a constant representing the water retention after all interpedal or gravitational, water has drained [hPa], and W_{miSat} and W_{maSat} are constants corresponding to the water content at which point the micropores and macropores are saturated, respectively [$\text{kg}_{\text{H}_2\text{O}}/\text{kg}_{\text{soil}}$]. Therefore, the field capacity is where $h = 330\text{hPa}$, and the permanent wilting point is the point at which $h = 15000\text{hPa}$. Equations [22] and [23] represent the water content at field capacity and permanent wilting point respectively.

$$\bar{W}_{FC} = \bar{W}_{mi(h=330)} + \bar{W}_{ma(h=330)} \quad [22]$$

$$\bar{W}_{WP} = \bar{W}_{mi(h=15000)} + \bar{W}_{ma(h=15000)} \quad [23]$$

The last step in calculating the AW is to convert the water content to volumetric (θ) from gravimetric (W) using the outlined equations [9] and [10]. Although this does

allow for accurate measurement of the classical definition of field capacity and permanent wilting point, it still fails to take into account the soil aggregation. These pressures (330 hPa for field capacity and 15,000 hPa for permanent wilting point) are experimentally based estimates for FC and WP. There is a need to determine the location and quantity of the water within the soil to be able to confidently say that the water is available to the plant for extraction.

Soil Shrinkage Curve Method

As explained earlier, field capacity and permanent wilting point are still primarily empirical quantities without a true physical definition and have been found by many different methods. Braudeau et al. (2005) proposed that these points can be extracted from the shrinkage curve (Figure 2). In the case of the permanent wilting point Braudeau et al. (2005) proposed that it physically refers to the point at which air begins to enter the micropores of the soil, while the field capacity correlates to the rapid decrease in water suction as the moisture content decreases. Therefore, they concluded that W_D was equal to field capacity and W_B was equivalent to the permanent wilting point (Figure 2) (Braudeau et al., 2005). Recalling equation [1], $AWC = \theta_{FC} - \theta_{WP}$, the available water could be calculated using these points. The issue with these conclusions is that they were based on statistical analysis rather than on a more developed realization of the thermodynamic interactions taking place within the soil. Consequently, a more accurate definition of the permanent wilting point could be stated as the water content at which the primary pedes are dry, and the field capacity could be defined as the physical point at which all interpedal (or gravitational) water has drained from the soil.

Since 2005, much progress has been made in understanding the internal thermodynamic interactions that occur within the soil medium. Assi et al. (2014) showed that \overline{W}_L , \overline{W}_M , and \overline{W}_N on the ShC are characteristic transition points that represent significant changes of the water pools within the soil. The authors concluded that W_L represents the volumetric water content at which all interpedal or gravitational water has drained out of the soil. Furthermore, \overline{W}_N was found to be representative of the point at which the primary pedes are dry (Assi et al., 2014; Braudeau et al., 2014a). Therefore, given the already established definitions of field capacity and permanent wilting point, it can be concluded that \overline{W}_L is equivalent to the field capacity and \overline{W}_N is the water content at the permanent wilting point. With this knowledge, equation [1] can be rewritten as equation [24].

$$AW = \frac{1}{\rho_w} \left(\frac{\overline{W}_L}{\overline{V}_L} - \frac{\overline{W}_N}{\overline{V}_N} \right) \quad [24]$$

where \overline{W}_L ($\propto \theta_{FC}$) and \overline{W}_N ($\propto \theta_{WP}$) are the water contents at point L and N, respectively [$\text{kg}_{\text{H}_2\text{O}}/\text{kg}_{\text{soil}}$], such that $\theta_{FC} = \overline{W}_L/\overline{V}_L\rho_w$ and $\theta_{WP} = \overline{W}_N/\overline{V}_L\rho_w$, \overline{V}_L and \overline{V}_N are the specific volumes of the soil at point L and N, respectively [$\text{dm}_{\text{soil}}^3/\text{kg}_{\text{soil}}$], and ρ_w is the specific density of water [$1 \text{ kg}_{\text{H}_2\text{O}}/\text{dm}_{\text{H}_2\text{O}}^3$]. In every case, the soil profile contains multiple horizons of soil that contain significantly different properties. For instance, a soil profile that contains an A horizon from 0 to 15 cm, an E horizon with a thickness of 15 cm (15-30 cm depth), and a B horizon at depths greater than 30 cm, would have a different field capacity and permanent wilting point in each horizon. This would significantly change the

available water in the entire profile. Therefore, to incorporate this element, each horizon must be included in the AW equation (equation [25]).

$$AW = \frac{1}{\rho_w} \left(\frac{\overline{W}_{LA}}{\overline{V}_{LA}} - \frac{\overline{W}_{NA}}{\overline{V}_{NA}} \right) + \frac{1}{\rho_w} \left(\frac{\overline{W}_{LE}}{\overline{V}_{LE}} - \frac{\overline{W}_{NE}}{\overline{V}_{NE}} \right) + \frac{1}{\rho_w} \left(\frac{\overline{W}_{LB}}{\overline{V}_{LB}} - \frac{\overline{W}_{NB}}{\overline{V}_{NB}} \right) \quad [25]$$

where \overline{W}_{LA} , \overline{W}_{LE} , and \overline{W}_{LB} represent the specific water content at point L for the A, E and B horizon, respectively, \overline{W}_{NA} , \overline{W}_{NE} , and \overline{W}_{NB} represent the specific water content at point N for the A, E and B horizon, respectively, \overline{V}_{LA} , \overline{V}_{LE} , and \overline{V}_{LB} represent the specific volume at point L for the A, E and B horizon, respectively, and \overline{V}_{NA} , \overline{V}_{NE} , and \overline{V}_{NB} represent the specific volume at point N for the A, E and B horizon, respectively.

2.2.4 Bulk Density

An important distinction to make between conventional methods and the hydro-structural evaluation is the normalization of all methods to report final outputs in volumetric water contents [$\text{m}^3_{\text{H}_2\text{O}}/\text{m}^3_{\text{soil}}$]. The wet bulk density is typically defined as the weight of soil at field capacity per total volume of soil, while dry bulk density is defined as the dry weight of soil per total volume of a soil sample taken at field capacity. In this sense, one may have a problem in defining the water content at field capacity once sampled from the field. In the cases of the FAO texture estimate and Saxon and Rawls' Pedotransfer functions, the units are already in volumetric dimensions so there is no need for a conversion. On the other hand, the pressure plate and water retention curve methods both report gravimetric water contents [$\text{kg}_{\text{H}_2\text{O}}/\text{kg}_{\text{soil}}$] and must be converted. In both cases, the soil's bulk density is conventionally utilized to determine the volumetric water content at permanent wilting point and field capacity using equations [26a] and [26b]:

$$\theta_{FC} = \overline{W}_{FC} \left(\frac{\rho_t}{\rho_w} \right), \text{ and} \quad [26a]$$

$$\theta_{PWP} = \overline{W}_{PWP} \left(\frac{\rho_d}{\rho_w} \right); \quad [26b]$$

where θ_{FC} and θ_{PWP} are the volumetric water contents at field capacity and permanent wilting point, respectively [$\text{m}^3_{\text{H}_2\text{O}}/\text{m}^3_{\text{soil}}$], ρ_t and ρ_d are the wet and dry bulk density of the soil, respectively [$\text{kg}_{\text{soil}}/\text{m}^3_{\text{soil}}$], ρ_w is the specific density of water [$\text{kg}_{\text{H}_2\text{O}}/\text{m}^3_{\text{H}_2\text{O}}$], \overline{W}_{FC} is the gravimetric water content of the soil at field capacity [$\text{g}_{\text{H}_2\text{O}}/\text{g}_{\text{soil}}$], and \overline{W}_{PWP} is the gravimetric water content of the soil at the permanent wilting point [$\text{g}_{\text{H}_2\text{O}}/\text{g}_{\text{soil}}$]. Conventionally, the assumption is made that the bulk density remains constant throughout the entire course of soil shrinkage. The error made in this assumption is apparent after further examination: the volume recorded in the bulk density is the volume of the soil *plus* the volume of the water and pore space. Therefore, as the water evaporates and the soil shrinks, the volume would no longer be constant. This is where the specific volume (the inverse of the bulk density) can play a role. The specific volume is recorded for hundreds of water contents when measuring the WRC and ShC. Both of these curves are modeled using thermodynamic equations and therefore, the specific volume can be determined for any water content desired. Hence, the water content at field capacity and permanent wilting point for the pressure plate method, the tensiometer technique, and the soil shrinkage curve method can be converted to volumetric. In this way, all five methods can be properly compared.

2.2.5 Establishing Reference Values

In order to compare these different techniques, it is important to identify which methods produce the most reliable or most widely accepted results for reference. Schelle et al. (2013) state that the most reliable process for measuring moisture contents at wet to moderately dry soil is the evaporation method (Schelle, Heise, Janicke, & Durner, 2013). The evaporation method is equivalent to the “water retention curve” method. Therefore, the water retention curve water content value will be used as the reference for the field capacity (330 hPa). On the other hand, the permanent wilting point has proven to be a greater challenge to accurately measure. Therefore, the most widely accepted method, the pressure plate method, will be used as reference. This will help to compare the results that are obtained.

3. MATERIALS AND METHODS

3.1 Sample Collection and Preparation

Two horizons of a soil profile were used for comparing the five methods. These were collected from the Millican Reserve in Millican, TX. As a variety of vegetable plants are cultivated on the Reserve, samples of the soil were taken at depths between 0-16 cm and 16-50 cm to account for the Ap (0-16 cm) and E (16-50) Horizons. Four undisturbed cylindrical samples (5 cm diameter by 5 cm height) from each horizon were used for analysis in the TypoSoil™. The cylindrical samples were obtained using a hand sampler with extensions to reach the second horizon. Before inserting the sampler, water was poured on the soil to saturate it. Vaseline was applied to the inside of the metallic cylindrical rings to ensure that the soil would come out of the rings with minimal resistance. These cores were air-sealed with plastic lids and transported to the laboratory for testing. Additionally, a 50 cm deep soil core measuring 2 inches in diameter was collected and taken to a certified soil characterization laboratory for measuring basic soil properties. In the lab, the core was divided into individual horizons to ensure that the horizon properties would not mix and ground and sieved to 2 mm. The ground and sieved soil was used to determine the particle size distribution (% sand, % clay), the organic matter, and used on the pressure plate to determine the water contents at 330 and 15,000 hPa. The field from which the samples were taken consisted of a Chazos loamy fine sand soil that had been plowed for cultivation.

The Chazos loamy fine sand soil (fine, smectitic, thermic Udic Palustalfs) is formed from loamy and clayey sediments consisting of deep, moderately well drained,

and slowly permeable soil. It is located on level to moderately sloping stream terraces. The majority of this soil series is designated for pasture, but some is used to grow vegetation and crops. The plot used in this experiment will be used for cultivation of multiple fruits and vegetables on a small farm (approximately one acre). Given the nature of the plants to be grown on this plot of land, only the top two horizons (Ap and E) will be considered in this study. (USDA, 2016)

(1) Horizon Ap is typically a thin horizon from 0 to 16 cm consisting of dark brown (10YR 4/3) loamy fine sand. It has a weak fine granular structure that is slightly hard and friable.

(2) Horizon E is generally composed of yellowish brown (10YR 5/4) loamy fine sand from a depth of 22 to 50 cm. It is a single grained horizon with a slightly hard and very friable structure.

Below the E horizon there are six more horizons: B_{t1}, B_{t2}, B_{t3}, B_{tk}, BC_{t1}, and 2BC_{t2}. Given that this study focuses on small plant rooting depths, none of the B horizons will be evaluated. (USDA, 2016)

The two structured soils that were tested, Rodah and Versailles, were the same used in Braudeau et al. (2014a). The Rodah soil is considered to be one of the most productive soils used for cultivation in the State of Qatar and has the texture classification of silty clay loam (Braudeau et al., 2014a). Three Rodah reconstituted top soil (0-15 cm depth) samples were analyzed for this study. Furthermore, one Versailles top soil (0-20 cm depth) sample was evaluated. This silt loam soil is native to France and was gathered, dried, sieved (2-mm), and reconstituted before being run in the TypoSoil™ (Assi et al., 2014; Braudeau et al., 2014a).

3.2 Soil Characterization Laboratory Measurements

Determining water contents at both 330 hPa and 15,000 hPa using the pressure plate method, procedures outlined by Richards (1965) and NRCS (1996) were utilized (NRCS, 1996; Richards, 1965). To summarize the procedures used, the sample was placed on the pressure plate and saturated with distilled water. Following this, the chamber of the pressure plate was slowly filled with N₂ until the pressure regulator was at 220 lbs/sq in pressure. After three days in this condition, the sample was removed and immediately weighed. Lastly, the dry weight was obtained by drying the sample overnight at 105°C and weighing the oven dried sample. Then the percent water was calculated using equation [27]:

$$\bar{W}_{15\ bar} = \frac{W_{15\ bar} - M_s}{M_s} \quad [27]$$

where $\bar{W}_{15\ bar}$ is the fraction of water content per soil at 15 bar tension [kg_{H₂O}/kg_{soil}], $W_{15\ bar}$ is the weight of the sample at 15 bar tension [kg_{H₂O+solid}], and M_s is the dry mass of the sample drying at 105°C overnight [kg_{solid}]. The same process was followed for measuring the water content at 330 hPa. Each process for the 330 hPa and 15,000 hPa were run on two separate soil samples and the results from the two runs were averaged.

Particle size distribution was recorded as a percentage of total sample mass for sand, silt, and clay. The procedures followed for determining particle size distribution were adopted from Kilmer and Alexander (1949) and Steele and Bradfield (1934) utilizing a pipet (Kilmer & Alexander, 1949; Steele & Bradfield, 1934).

Lastly, organic matter mass percentage was determined by finding the percent of organic carbon present in the sample and converting to organic matter. The conversion

was carried out by the commonly used practice of using the value of 1.724 such that (Lunt, 1931; Read & Ridgell, 1922):

$$OM(\%) = 1.724 \times OC(\%) \quad [28]$$

where $OM(\%)$ the percent organic matter of the total sample mass [$\text{kg}_{\text{OM}}/\text{kg}_{\text{total}}$] and $OC(\%)$ is the percent organic carbon of the total sample mass. Organic carbon percentage was experimentally determined by using a tube furnace and a scrubbing train following the procedures of NRCS (1996) and Nelson and Sommers (1982) (Nelson & Sommers, 1982; NRCS, 1996).

3.3 Finding Bulk Density

As discussed, the specific volume was used in this study rather than the bulk density according to equations [29a] and [29b]:

$$\rho_t = \frac{1}{\bar{V}_t} \quad [29a]$$

$$\rho_d = \frac{1}{\bar{V}_d} \quad [29b]$$

Where ρ_t is the soil bulk density at field capacity (330 hPa or \bar{W}_L) [$\text{g}_{\text{soil}}/\text{cm}^3$], d is the soil bulk density at the permanent wilting point (15,000 hPa or \bar{W}_N) [$\text{g}_{\text{soil}}/\text{cm}^3$], \bar{V}_t is the specific volume of the soil at field capacity (330 hPa or \bar{W}_L) [$\text{g}_{\text{soil}}/\text{cm}^3$], and \bar{V}_d is the specific volume of the soil at the permanent wilting point (15,000 hPa or \bar{W}_N) [$\text{g}_{\text{soil}}/\text{cm}^3$].

3.4 Measuring Shrinkage Curve and Water Retention Curve

The samples were collected in 5 cm diameter and 5 cm height rings that contained only one horizon each. They were then placed on a sand box bath to saturate them by capillary wetting. The water in the bath was maintained at 2 cm below the bottom of the

sample. Assi et al. (2014) described in detail the methods for preparation and measuring of the soil samples to obtain the shrinkage curve (ShC) and water retention curve (WRC) using the TypoSoil™ (Assi et al., 2014). Every eight minutes, the device simultaneously measured the mass, diameter, height, and pressure within the soil of each sample. A total of eight samples could be run in the TypoSoil™ at one time. For the Chazos soil, four replicates of the top two horizons were analyzed.

3.5 Determination of Hydro-Structural Parameters

The hydro-structural parameters listed in Table 2 and equations [11]-[18] were determined using an optimization routine as described by Assi et al. (2014) and Braudeau et al. (2016) by minimizing the sum of squares between the modeled and measured ShC and WRC. This procedure generates the best fitting of the modeled ShC and WRC with the raw measured data. The thermodynamic equations used for the modeling can then be solved for any water content higher than the measured data.

3.6 Quantification of Available Water

Following the procedures outlined in the theoretical background, the available water was quantified for the two different Chazos horizons of the soil by the five methods. Additionally, the FAO estimate, WRC, ShC methods were carried out for the Rodah and Versailles soils. Microsoft Excel was utilized for input of data and calculations in following the procedures outlined by Braudeau et al. (2016).

4. RESULTS AND DISCUSSION

4.1 Comparison of Techniques

The procedures described above were carried out for all techniques on all four soil types. For consistency, the wet bulk density (or the specific volume at the water content of the field capacity) was used for unit conversion of the pressure plate, tensiometer, and

MR - Ap	Specific Volume		Bulk Density	
	Wet	Dry	Wet	Dry
PP	0.694 ± 0.003	0.693 ± 0.003	1.440 ± 0.006	1.443 ± 0.006
WRC	0.694 ± 0.003	0.693 ± 0.003	1.441 ± 0.007	1.443 ± 0.005
ShC	0.702 ± 0.001	0.693 ± 0.002	1.424 ± 0.002	1.442 ± 0.005
MR - E	Specific Volume		Bulk Density	
	Wet	Dry	Wet	Dry
PP	0.677 ± 0.004	0.677 ± 0.004	1.477 ± 0.008	1.477 ± 0.008
WRC	0.677 ± 0.004	0.677 ± 0.004	1.477 ± 0.008	1.477 ± 0.008
ShC	0.679 ± 0.004	0.677 ± 0.004	1.472 ± 0.004	1.477 ± 0.008
Rodah	Specific Volume		Bulk Density	
	Wet	Dry	Wet	Dry
PP	-	-	-	-
WRC	0.900 ± 0.001	0.849 ± 0.002	1.111 ± 0.001	1.178 ± 0.003
ShC	0.946 ± 0.006	0.846 ± 0.002	1.057 ± 0.006	1.183 ± 0.003
Versailles	Specific Volume		Bulk Density	
	Wet	Dry	Wet	Dry
PP	-	-	-	-
WRC	0.721	0.674	1.388	1.483
ShC	0.735	0.676	1.361	1.480

Table 3: Wet and dry specific volume and bulk density for all four soil types

shrinkage curve methods (table 3). Each value includes the standard deviation with the exception of the Versailles soil as there was only one sample used for calculations.

Using the particle size distribution analysis, it was found that both the Ap and E horizons were loamy fine sands (lfs). Additionally, the Rodah sample was a silty clay loam (sicl) and the Versailles was a silt loam (sil). Therefore, taking the average of the ranges for field capacity and permanent wilting point from table 1 for each texture, we were able to estimate the water content at each of these vital soil-water states. In order to solve the Pedotransfer functions for the Millican samples, it was necessary to find the percentage of sand particles, clay particles and organic matter. It was found that the Ap horizon contained 82.9% sand particles, 3.9% clay particles, and 1.30% organic carbon. The organic carbon was converted to organic matter to get 0.022% organic matter in horizon Ap. These percentages were converted to decimals and then equations [3]-[6] were used to obtain final values. Similarly, the E horizon was found to contain 83.7% sand particles, 2.9% clay particles, and 0.13% organic carbon (or 0.002% organic matter). The pressure plate method produced water content percentages of 9.7% and 4.5% for pressures of 330 hPa and 15,000 hPa, respectively, for the MR-Ap sample. Additionally, the MR-E sample was found to have water content percentages of 5.6% and 1.8% for 330 hPa and 15,000 hPa, respectively. Gravimetric water content values were extracted from the water retention curve (WRC) that represented the internal pressure correlating to the field capacity (330 hPa) and permanent wilting point (3754 hPa). Three WRC were used for the MR-Ap, MR-E, and Rodah soils while only one sample was used for the Versailles soil (figures 9-16). The reason for only using three of the four samples from the MR-Ap and

MR-E batches was that there was one sample in each batch that did not yield full results making it difficult to model. The same samples were used for the soil shrinkage curve method for extracting the parameters \overline{W}_L and \overline{W}_N . A conversion was carried out using the bulk densities summarized in table 3 for the pressure plate method (PP), the water retention method (WRC), and the soil shrinkage curve method (ShC). The results with their standard deviations are summarized in tables 4-7 and figures 5-8. Note the reason for there being no standard deviation for the pedotransfer functions in tables 4 and 5 was that the numbers were only measured once. It is important, however, to keep in mind the uncertainties of these outputs due to their low coefficient of determinations as mentioned in the theoretical

Horizon Ap	Category	Method	Field Capacity [m ³ H ₂ O/m ³ soil]	Wilting Point [m ³ H ₂ O/m ³ soil]	AW [m ³ H ₂ O/m ³ soil]
	Standard Methods	FAO Estimates	0.150 ± 0.040	0.065 ± 0.035	0.085 ± 0.038
		Pedotransfer Functions	0.073*	0.017*	0.055*
		Pressure Plates	0.140 ± 0.002	0.065 ± 0.002	0.077 ± 0.002
	Pedostructural Methods	WRC	0.144 ± 0.004	0.031 ± 0.003	0.113 ± 0.003
		ShC	0.332 ± 0.003	0.075 ± 0.012	0.258 ± 0.009

Table 4: MR-Ap soil samples summary of five methods

Horizon E	Category	Method	Field Capacity [m ³ H ₂ O/m ³ soil]	Wilting Point [m ³ H ₂ O/m ³ soil]	AW [m ³ H ₂ O/m ³ soil]
	Standard Methods	FAO Estimates	0.150 ± 0.040	0.065 ± 0.035	0.085 ± 0.038
		Pedotransfer Functions	0.065*	0.010*	0.055*
		Pressure Plates	0.082 ± 0.003	0.027 ± 0.003	0.055 ± 0.003
	Pedostructural Methods	WRC	0.064 ± 0.003	0.008 ± 0.003	0.056 ± 0.003
		ShC	0.282 ± 0.004	0.034 ± 0.004	0.247 ± 0.004

Table 5: MR-E soil samples summary of five methods

background. Additionally, the Versailles soil does not have any standard deviation on the pedostructural methods because only one sample was analyzed to determine the outputs.

Rodah	Category	Method	Field Capacity [m ³ _{H2O} /m ³ _{soil}]	Wilting Point [m ³ _{H2O} /m ³ _{soil}]	AW [m ³ _{H2O} /m ³ _{soil}]
	Standard Methods	FAO	0.335 ± 0.035	0.205 ± 0.035	0.130 ± 0.035
	Pedostructural Methods	WRC	0.258 ± 0.001	0.126 ± 0.001	0.132 ± 0.001
ShC		0.426 ± 0.017	0.109 ± 0.005	0.317 ± 0.012	

Table 6: Rodah soil samples summary with averages and standard deviations

Versailles	Category	Method	Field Capacity [m ³ _{H2O} /m ³ _{soil}]	Wilting Point [m ³ _{H2O} /m ³ _{soil}]	AW [m ³ _{H2O} /m ³ _{soil}]
	Structural Methods	FAO	0.290 ± 0.070	0.150 ± 0.060	0.140 ± 0.065
	Pedostructural Methods	WRC	0.297*	0.086*	0.210*
ShC		0.408*	0.065*	0.343*	

Table 7: Versailles soil sample summary with averages and standard deviations

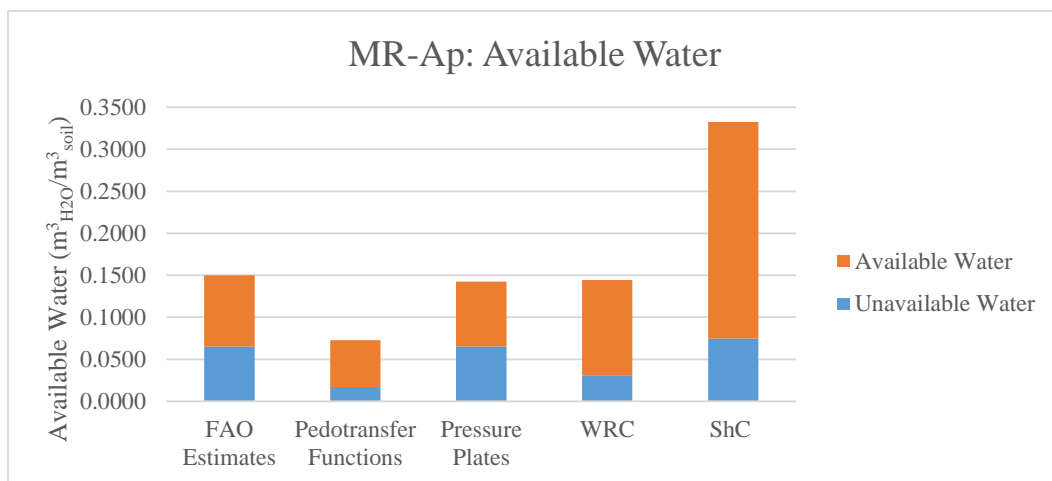


Figure 5: Available water comparison for MR-Ap

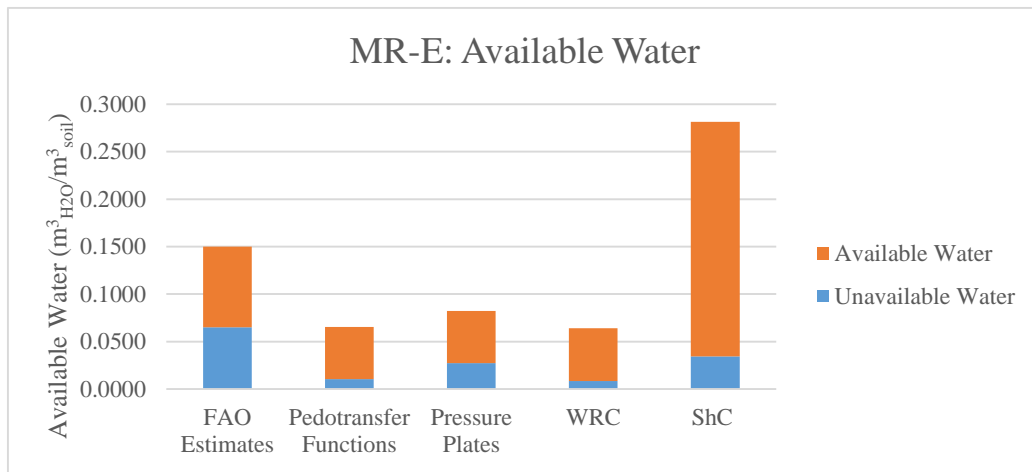


Figure 6: Available water comparison for MR-E soil

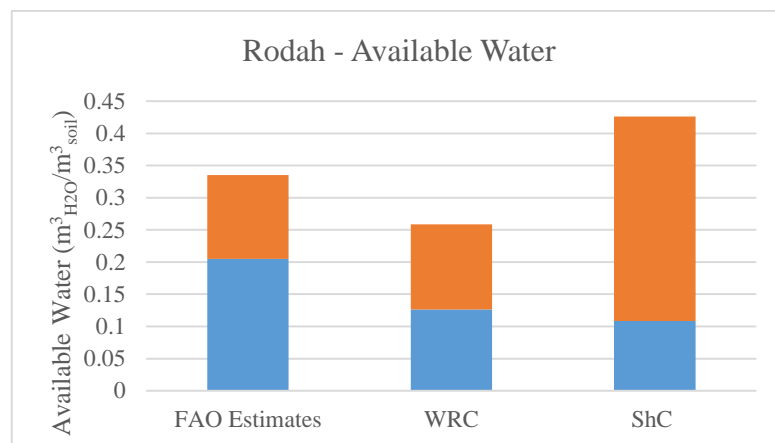


Figure 7: Available water comparison for Rodah

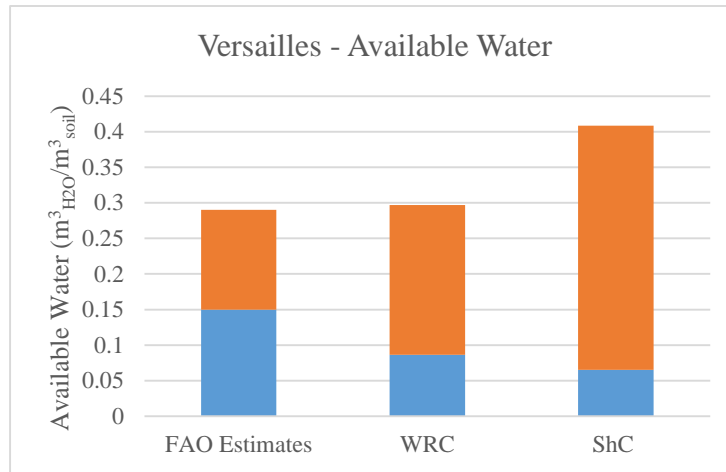


Figure 8: Available water comparison for Versailles

These results and figures help bring into focus the main conclusions that can be identified from this study. In particular, the pedostructural evaluation of the soil using the ShC transition points of \overline{W}_L and \overline{W}_N , is significantly higher than any of the other estimations. This does not necessarily lead to the conclusion that there is more water holding capacity in the soil, but rather that this large discrepancy should lead to questioning the standard and pedostructural methods for validity. For instance, in the case of the ShC evaluation of the soil in the Millican samples, the upper portion of the curve is difficult to measure when the slope of the interpedal water is not easily identifiable. In figure 11, it is clear that there is very little interpedal water and, therefore, it becomes

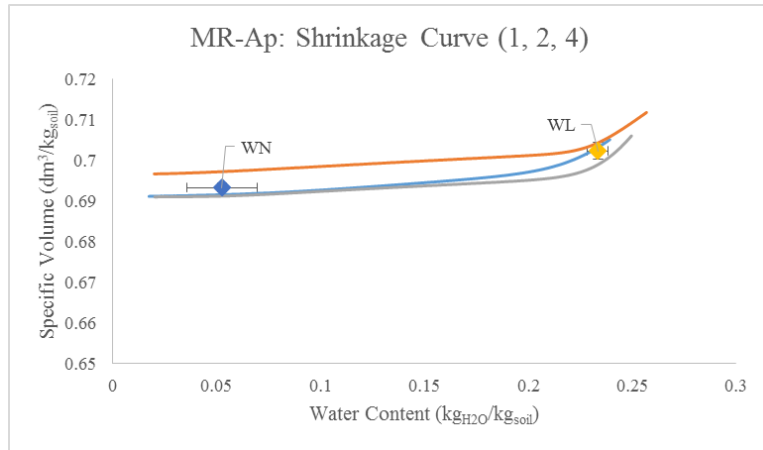


Figure 9: MR-Ap shrinkage curves used with average WL and WN plotted (error bars for WL are on the order of the size of the symbol)

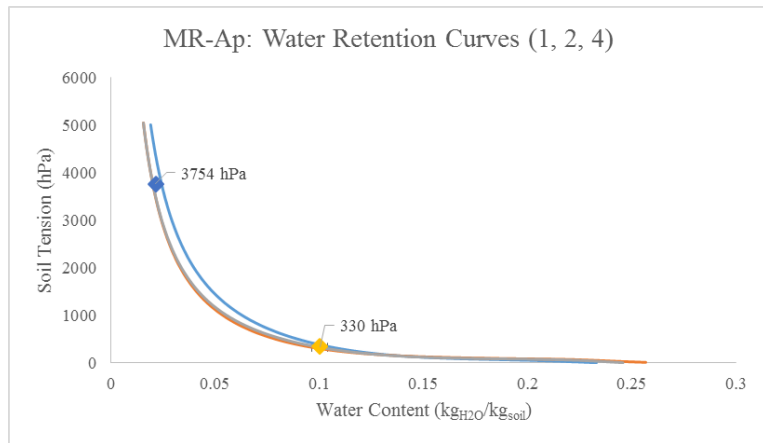


Figure 10: MR-Ap water retention curves with average FC and WP plotted (error bars are on the order of the size of the symbol)

difficult to determine exactly where \overline{W}_L falls on the curve. Therefore, it is the applicability and certainty of this data is limited. In the same way, figure 9 shows that \overline{W}_L is much higher on the transition than would be expected under merely visual inspection. Therefore,

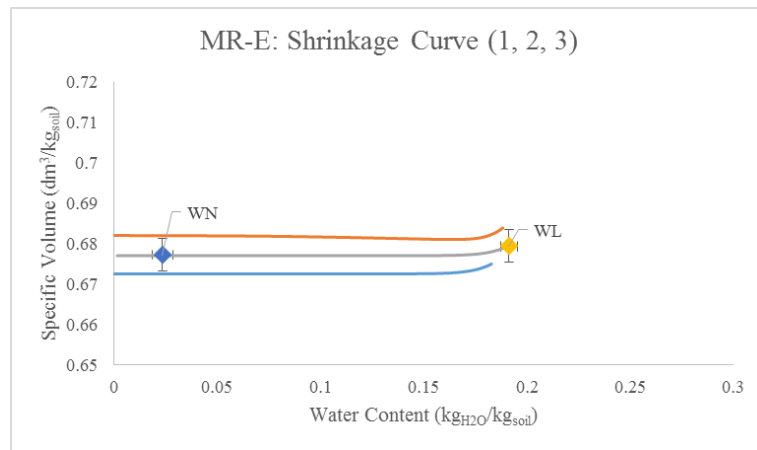


Figure 11: MR-E soil shrinkage curves with average WL and WN plotted

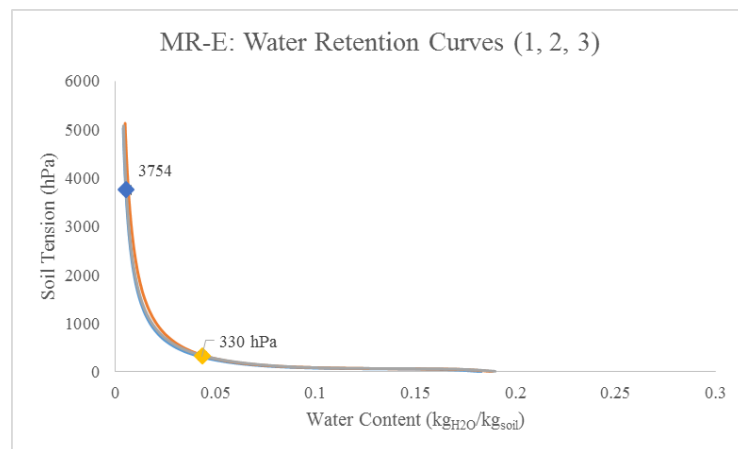


Figure 12: MR-E water retention curves with average FC and WP plotted (error bars are on the order of the size of the symbol)

when drawing conclusions it is important to take into account the aforementioned potential errors within the analysis for the pedostructural shrinkage curve.

Another interesting point, is the accuracy with which the FAO values estimate the field capacity and permanent wilting point in the Ap horizon, and how poorly they estimate

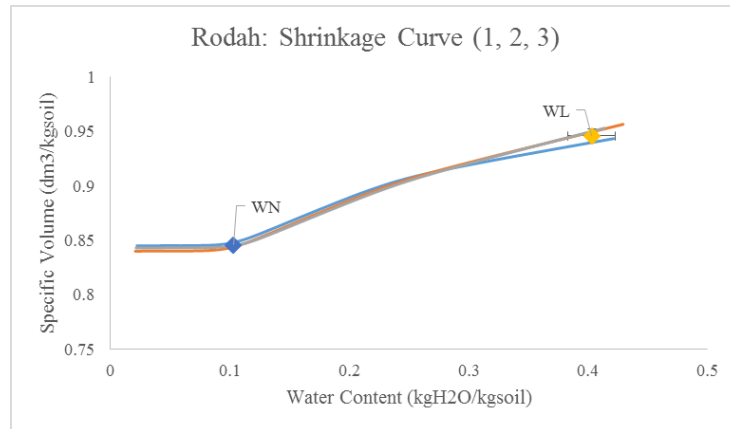


Figure 13: Rodah soil shrinkage curves with average WL and WN plotted (error bars are on the order of the size of the symbol)

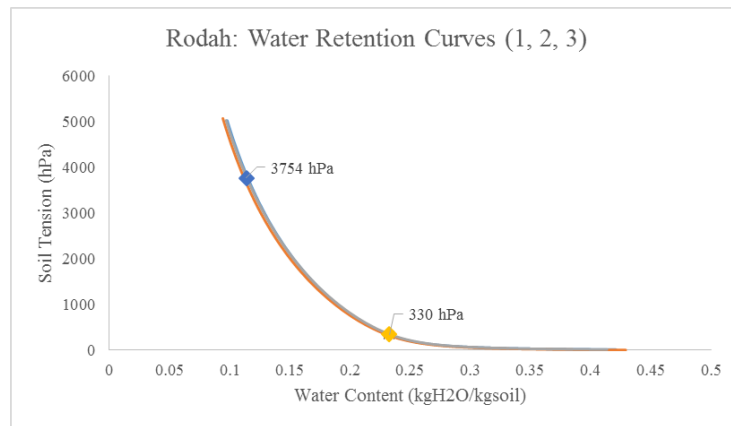


Figure 14: Rodah water retention curves with average FC and WP plotted (error bars are on the order of the size of the symbol)

them in the E horizon. This is a good demonstration of why using the average of the FAO range of values for FC and WP is dangerous.

Given the relative agreement between the four methods other than the ShC, it was important to evaluate different types of soils, particularly well-structured soils, to investigate the large discrepancy in measurements that the ShC method produced. Therefore, the Rodah and Versailles soils (from Assi et al., 2014; and Braudeau et al., 2014a) were used and the results obtained for the FAO estimate, WRC, and ShC are

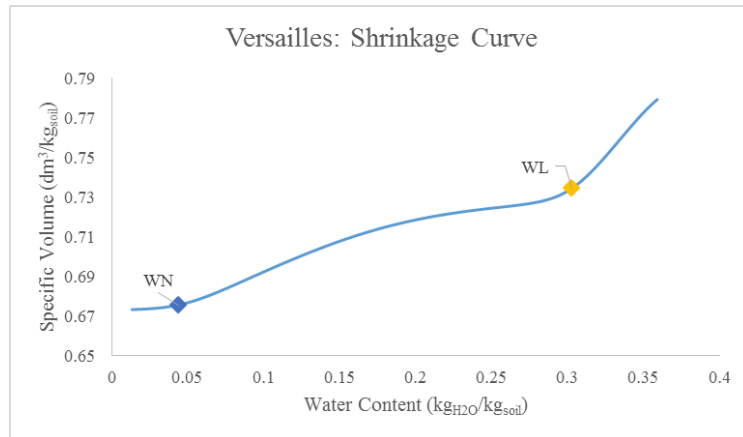


Figure 15: Versailles soil shrinkage curve with WL and WN plotted

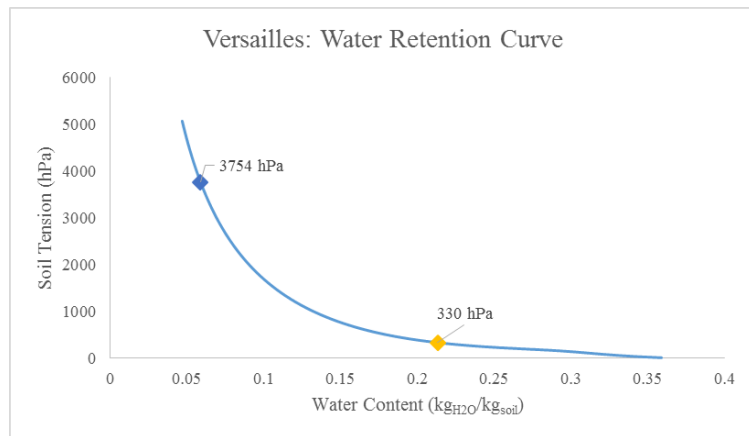


Figure 16: Versailles water retention curve with FC and WP plotted

summarized in table 6 and 7. The field capacity is the most important parameter considered in the table, due to the good agreement on the lower end of ShC with the WRC method (see tables 6 and 7). One of the most significant differences between the data set for the Versailles and the two Texas soils is that there is significant interpedal water. When this water is present, it becomes easier to identify and model the upper portion of the ShC and, consequently, becomes much easier to pinpoint \overline{W}_L . This could be one reason why the

field capacity estimated by the ShC for the Versailles soil is closer to the estimate produced from the WRC.

Another observation that can be made from all four of the soils analyzed in this study is the consistency with which the 330 hPa point falls on the WRC. This point, as described by Braudeau et al. (2005), is the transition between the macro water and the micro water in the soil. Further work could involve testing to see whether or not this pattern holds true for other types of soil as well.

4.2 Varying Bulk Density

As discussed within the theoretical background, the assumption of a constant bulk density throughout the different water contents of the soil could lead to inaccuracies in determining field capacity and permanent wilting point. Both pedostructural methods (water retention curve and the soil shrinkage curve) use the specific volume to find the volumetric water content of the soil at FC and WP. To investigate the impact of assuming a constant bulk density throughout the shrinkage of a soil, a comparison was done to evaluate the difference between using the wet bulk density for both the field capacity and

the permanent wilting point and using the wet and dry bulk densities for the field capacity and wilting point, respectively (table 8).

Soil	Technique	Bulk Density Use	Available Water [m ³ _{H₂O} /m ³ _{soil}]	Percent Decrease [%]
MR-Ap	ShC	Wet	0.258	0.37%
		Wet/Dry	0.257	
MR-Ap	WRC	Wet	0.114	0.04%
		Wet/Dry	0.113	
MR-E	ShC	Wet	0.247	0.04%
		Wet/Dry	0.247	
MR-E	WRC	Wet	0.056	0.00%
		Wet/Dry	0.056	
Rodah	ShC	Wet	0.317	4.07%
		Wet/Dry	0.304	
Rodah	WRC	Wet	0.132	5.79%
		Wet/Dry	0.124	
Versailles	ShC	Wet	0.352	1.49%
		Wet/Dry	0.347	
Versailles	WRC	Wet	0.214	2.60%
		Wet/Dry	0.209	

Table 8: Impact of using a constant bulk density vs. wet and dry bulk density

It can be seen from table 8 that for sandy soil (MR-Ap and MR-E) the impact of using a constant bulk density is negligible. However, it is also evident that well-structured soils are negatively impacted when considering a changing bulk density. Again, the issue of the bulk density is mainly related to how accurate we are in defining the water content at field capacity. For example, the Rodah soil analyzed by the WRC shows a 5.79% decrease in available water. Assuming an average depth of 1 meter for a root it can be seen that there would be 8 mm less water available to the plant than if the bulk density was assumed constant. Given an average farm size in Texas to be 500 acres (2,023,000 m²),

there is the potential to over irrigate; using approximately 16,000 m³ more water than necessary. This water will either percolate through the soil or be evaporated before ever being used by the plant. With precision irrigation and water conservation becoming increasingly important, knowing the exact amount of water that the soil can hold becomes even more vital.

4.3 Summary of the Methods Used

Table 9 investigates the strengths and weaknesses of each method evaluated in this study. It can be seen that the pros and cons of these theories vary widely, and must be taken into consideration when deciding which method to use for determining the water holding of a soil.

<i>Method</i>	<i>Strengths</i>	<i>Weaknesses</i>
FAO Estimate	<ul style="list-style-type: none"> • No need for lab work • Thorough data set • Could be very accurate 	<ul style="list-style-type: none"> • Must texture in field if no lab work is done • Values given in range are fairly wide and must make an educated guess on which to use • Could be very inaccurate
Pedotransfer function	<ul style="list-style-type: none"> • Accurate estimate with minimal lab work needed • Exact soil tested 	<ul style="list-style-type: none"> • Must take exact soil to lab for testing • Limited predictive accuracy based on statistical analysis
Pressure Plate	<ul style="list-style-type: none"> • Accurate estimate especially on the lower end (WP) • Exact soil tested 	<ul style="list-style-type: none"> • Must take exact soil to lab for testing • Lab work is extensive
Water Retention Curve	<ul style="list-style-type: none"> • Accurate measurement of internal tension up to ~1000 hPa • Can be accurately extended for higher values of internal tension • Helps to identify behavior of the soil 	<ul style="list-style-type: none"> • Exact measurements only go up to ~1000 hPa • Modeling of extended WRC for higher values of internal water retention can be erroneous if measurements for <1000 hPa are inaccurate • Instrumentation used needs careful preparation for satisfactory results
Soil Shrinkage Curve	<ul style="list-style-type: none"> • Macro and Micro water pools can be established • Gives Physical visual of behavior of the soil • With good data, points can be quickly and easily determined 	<ul style="list-style-type: none"> • Non-well-structured soils are difficult to analyze • Upper portion of the ShC can be difficult to accurately measure

Table 9: Comparison of strengths and weaknesses

5. CONCLUSIONS

This paper lays out a clear methodology for estimating the available water within the soil using the new pore structure concept. By using hydro-structural parameters extracted from the soil shrinkage curve it was possible to relate the soil aggregation and water interactions to the water holding. Although there are questions regarding the validity of the hydro-structural parameters chosen on the shrinkage curve, the possible impact of the outcomes could be significant. The fact that the new methods examined in this paper raise legitimate questions, could mask its enormous potential impact on agricultural water management. Therefore, it is important to validate this theory by testing more soils with different mineralogy and texture to ensure that the pattern seen in this research holds under varying conditions.

By demonstrating the application of this new methodology on multiple soil types a few conclusions could be drawn. One such conclusion is the good agreement between the standard methods and the water retention method. Another major conclusion to be drawn from this study is that bulk density should *not* always be assumed to be constant, especially with non-sandy soils. Moreover, it may be a good estimation to use the wet bulk density in measuring the field capacity, but the question in this research remains unanswered. How can we accurately measure or identify the field capacity? This research worked on identifying a measurable point in both water retention curve and shrinkage curve to identify the field capacity value. This point considers the soil aggregate structure and its thermodynamic interaction with water. Therefore, this soil evaluation work makes it apparent that there is a definite shift in the ratio of dry weight of soil per unit volume of

soil plus pores plus water and therefore, that there is also a shift in bulk density throughout the shrinking of the soil. This result is more significant in a soil with high amounts of shrinkage as the Rodah and Versailles samples showed.

One thing that became clear in this study is that there are both advantages and disadvantages for each method discussed within this paper. In the case of the standard methods, it was evident that the historical reliability of laboratory measurements have helped to make these methods publically acceptable in the scientific community. However, it was observed that the statistical or empirically-based values and assumptions made about a constant bulk density weaken the validity of this methods. On the other hand, the pedostructural methods offer a new way of thinking about soil-water interaction and quantification based on the physical behavior of the soil. Nonetheless, the sample size and lack of field-testing cause the results from the pedostructural methods to be questioned for consistency and reliability. Overall, it can be concluded that the pedostructure concept has opened up new avenues for research and investigation in soil-water that could have an enormous impact on agricultural water management.

REFERENCES

- Allen, R. G., Pereira, L. S., Raes, D., & Smith, M. (1998). Crop evapotranspiration: Guidelines for computing crop requirements. Irrigation and Drainage Paper No. 56, FAO, (56), 300. <http://doi.org/10.1016/j.eja.2010.12.001>
- Assi, A. T., Accola, J., Hovhannissian, G., Mohtar, R. H., & Braudeau, E. (2014). Physics of the soil medium organization part 2 : pedostructure characterization through measurement and modeling of the soil moisture characteristic curves. *Front. Environ. Sci.*, 2(March), 1–17. <http://doi.org/10.3389/fenvs.2014.00005>
- Bellier, G., & Braudeau, E. (2013). Device for Measurement Coupled with Water Parameters of Soil. World Intellectual Property Organization, European Patent Office. <http://doi.org/US 2010/0311130 A1>
- Bittelli, M., & Flury, M. (2009). Errors in Water Retention Curves Determined with Pressure Plates. *Soil Science Society of America Journal*, 73(5). <http://doi.org/10.2136/sssaj2008.0082>.
- Braudeau, E., Assi, A. T., & Mohtar, R. H. (2016). *Hydrostructural Pedology*. ISTE Ltd and John Wiley & Sons, Inc.
- Braudeau, E. F., & Mohtar, R. H. (2014). A Framework for Soil-Water Modeling Using the Pedostructure and Structural Representative Elementary Volume (SREV) Concepts. *Frontiers in Environmental Science*, 2(June), 1–13. <http://doi.org/10.3389/fenvs.2014.00024>
- Braudeau, E., Hovhannissian, G., Assi, A. T., & Mohtar, R. H. (2014a). Soil water thermodynamic to unify water retention curve by pressure plates and tensiometer. *Hydrosphere*, 2(October), 30. <http://doi.org/10.3389/feart.2014.00030>.
- Braudeau, E., Assi, A., Bouckcim, H. & Mohtar, R.H. (2014b). Physics of the soil medium organization part 1 : thermodynamic formulation of the pedostructure water retention and shrinkage curves. *Front. Environ. Sci.*, 2(March), 1–17. <http://doi.org/10.3389/fenvs.2014.00004>.
- Braudeau, E., & Mohtar, R. H. (2009). Modeling the soil system: Bridging the gap between pedology and soil-water physics. *Global and Planetary Change*, 67(1–2), 51–61. <http://doi.org/10.1016/j.gloplacha.2008.12.002>
- Braudeau, E., Sene, M., & Mohtar, R. H. (2005). Hydrostructural characteristics of two African tropical soils. *European Journal of Soil Science*, 56(3), 375–388. <http://doi.org/10.1111/j.1365-2389.2004.00679x>.

- Braudeau, Erik; Frangi, Jean-Pierre; Mohtar, R. (2004). Characterizing Nonrigid Aggregated Soil-Water Medium Using its Shrinkage Curve. *Soil Science Society of America Journal*, 68(2), 359–370. <http://doi.org/10.2136/sssaj2004.3590>
- Brewer, R. 1964. *Fabric and mineral analysis of soils*. John Wiley and Sons (Eds), New York. 482 pp.
- Hudson, B. D. (1994). Soil organic matter and available water capacity. *Journal of Soil and Water Conservation*, 49(2), 189–194.
- Kilmer, V. J., & Alexander, L. T. (1949). Methods of Making Mechanical Analyses of Soils. *Soil Science*, 68(1), 15–24. <http://doi.org/10.1097/00010694-194907000-00003>
- Lunt, H. (1931). The carbon-organic matter factor in forest soil humus. *Soil Science*, 32(1), 27–34.
- Nelson, D. W., & Sommers, L. E. (1982). Total carbon, organic carbon and organic matter. In A.L. Page. *Method of Soil Analysis. Part II*. (2nd ed.).
- NRCS. (1996). *Soil Survey Laboratory Methods Manual*, (42), 716. <http://doi.org/10.1021/ol049448l>
- Read, J. W., & Ridgell, R. H. (1922). On the use of the conventional carbon factor in estimating soil organic matter.pdf. *Soil Science*, 13, 1–6.
- Richards, L. A. (1941). *Soil moisture tensiometer materials and construction*. U.S. Department of Agriculture. <http://doi.org/10.1097/00010694-194204000-00001>
- Richards, L. A. (1948). Porous plate apparatus for measuring moisture retention and transmission by soil. *Soil Science*. <http://doi.org/10.1097/00010694-194808000-00003>
- Richards, L. A. (1965). Physical Condition of Water in Soil. In C.A. Black (ed.) *Methods of Soil Analysis Part 1*.
- Richards, L. A., & Gardner, W. (1936). Tensiometers for measuring the capillary tension of soil water. *Journal of the American Society of Agronomy*, 28(5), 352–358.
- Saxton, K., & Rawls, W. (2006). Soil Water Characteristic Estimates by Texture and Organic Matter for Hydrologic Solutions. *Soil Science Society of America Journal*, 70, 1569–1578. <http://doi.org/10.2136/sssaj2005.0117>

- Schelle, H., Heise, L., Janicke, K., & Durner, W. (2013). Water retention characteristics of soils over the whole moisture range: A comparison of laboratory methods. *European Journal of Soil Science*, 64(6), 814–821.
<http://doi.org/10.1111/ejss.12108>
- Singh, A. (2007). Integrated Water Management: Water and Plant Growth, 1–16.
- USDA. (2008). Available water capacity. *Soil Quality Indicators*, 501(June), 2008.
- USDA. (2016). USDA Soil Series. Retrieved from
<https://soilseries.sc.egov.usda.gov/osdname.aspx>